A Wireless Powered Implantable Bio-Sensor Tag System-on-Chip for Continuous Glucose Monitoring

Shuo Guan, Jingren Gu, Zhonghan Shen, Junyu Wang
State Key Lab of ASIC and System
Fudan University
Shanghai, China
junyuwang@fudan.edu.cn

Yue Huang, Andrew Mason
Department of Electrical and Computer Engineering
Michigan State University
East Lansing, USA
mason@msu.edu

***Abstract*—an implantable passive radio frequency identification (RFID) sensor tag system-on-chip (SoC) for glucose monitoring is developed in this paper. A high frequency RFID tag, a bio-sensor interface, as well as the electrodes are included in this chip. The signal of blood sugar level from the bio-sensor is detected and converted into digital data, and then the data is encrypted and transmitted to an RFID reader on top of the skin. To measure the weak current signals, a current readout circuit, a current splitter, an ADC and a potentiostat are designed in the chip. Correlated double sample (CDS) technology is used in the readout circuit to reduce the 1/f noise and the op-amp's offset. The chip is taped out in SMIC 0.13 μm CMOS process. Simulation results show that the system can measure weak current signals in the range of 10 fA-100 pA.**

***Index Terms*—Sensor interface circuit, RFID, glucose monitoring, signal processing.**

I. INTRODUCTION

Traditionally, people with type I diabetes measure their blood sugar level by a finger prick test. But the spot measurements cannot guarantee that there is no excursion of a person's blood sugar outside of the normal physiological range. Research shows that continuous blood glucose monitoring can help reduce more than 40% of the symptoms associated with diabetes [1] [2]. A promising approach of continuous glucose monitoring is to implant a glucose sensor along with a wireless micro-system in the human body [3] [4]. For this to work, a small implant with an accurate and rapid blood glucose sensing component and an efficient radio frequency module plays a key role. Furthermore, since the glucose level is to be transmitted to a receiver outside of the body in a wireless way, the privacy of the patient needs to be protected.

This paper proposes an implantable system on chip (SoC) which includes a fully functional high frequency (HF, 13.56 MHz) RFID tag, a glucose sensor interface and on-chip electrodes. The data acquisition (DAQ) unit in the bio-sensor interface can work in four different ranges through the change of working frequency and can measure weak current signals in the range of 10 fA-100 pA. A passive HF RFID system based on ISO/IEC 15693 protocol [5] is designed, and the Hummingbird cryptography algorithm [6] is implemented in the baseband to encrypt the glucose data before it is sent out to the RFID reader wirelessly.

This work was sponsored by the National Natural Science Funds of China (61076022), the National High Technology Research and Development Program("863"Program) of China (2011AA100701) and the Shanghai Pujiang Program. Corresponding author: Junyu Wang.

II. SYSTEM ARCHITECTURE AND WORKING FLOW

A. System architecture

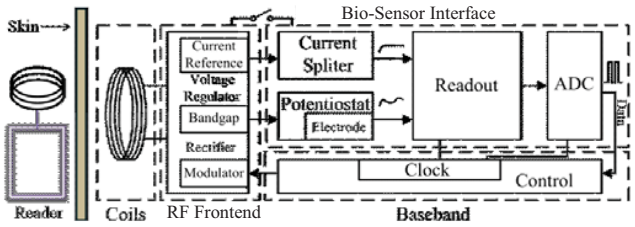

Fig. 1. Block diagram of the glucose sensor tag chip SoC

The implantable glucose sensor tag chip consists of a radio frequency (RF) frontend, a bio-sensor interface and a digital baseband (Fig. 1). The high frequency tag works passively and gain power from the RF energy of the reader. The high frequency band is selected since it is an industrial-scientific-medical (ISM) frequency band and it performs better for implant in vivo than ultra high frequency band. The RF frontend rectifies and transforms the received RF-signal to the DC supply voltage and provide power for the baseband and the bio-sensor interface. In the bio-sensor interface, a current splitter is designed to provide the reference current for gain calibration and currents in different detection ranges for testing purpose. The DAQ module, including a potentiostat and a readout circuit, is designed to detect, amplify and transform the reacting current (included with information of blood sugar concentration) into a voltage signal. An ADC converts the voltage signal into a digital signal and transmits it into baseband for data processing. In baseband, the data will be encrypted by a cryptographic engine based on the Hummingbird Algorithm before being sent out to the RFID reader.

B. Work flow of the sensor tag chip

The sensor tag chip works according to the following flow: 1) the reader outside of the body queries the sensor tag using commands conforming to ISO/IEC 15693 protocol; 2) the baseband resets datum when it receives power-on-reset (PoR) signal; 3) the bio-sensor interface begins self-calibration when receiving a "power ready" signal from the front-end, which means the bio-sensor interface has enough power to work; 4) when the "inventory" signal is received from the reader, the

baseband enables the bio-sensor interface; 5) under the control of the potentiostat, reaction starts at the sensor. The principle of reaction is described in [7] and the bio-sensor is being researched by our partner. The reacting current is measured and the converted data is saved in the baseband. At the same time, the baseband shuts off the bio-sensor interface to save power; 6) the baseband encrypts the data stored and then sends it to the reader when the sensor tag receives the "send" command from the reader. The system repeats the above steps during every work cycle.

The self-calibration is designed to adjust system gain before detecting the weak signal. It is necessary since possible leakage and process variation, such as the fabrication error of the integrated capacitor, may lead to gain bias. For every power-on-reset, the system accomplishes a self-calibration and keeps the system gain modified until the system is powered off.

III. CIRCUIT IMPLEMENTATION

A. Front End

RF-Frontend is critical on the power acquisition and the communication of the whole chip. A RF-Frontend is made up of the following components: rectifier, LDO, band-gap, a clock extractor, a PoR module, a modulator and a demodulator (Fig.2). Considering the property of an implantable tag, buffers and overload protector are added in our design.

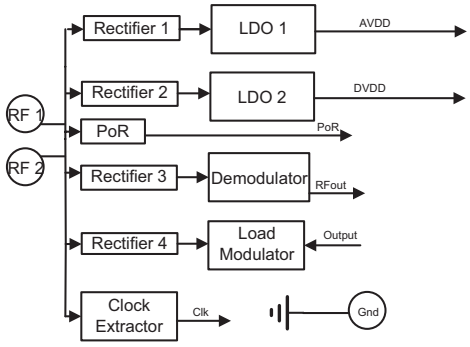

Fig. 2 Block diagram of RF-Front end

The source of analog circuits and the source of digital circuits are separated and powered by two rectifiers respectively. Note that, unlike the traditional bridge rectifier circuit, the rectifier in this paper replaces the input of the second stage from self bias to the output of two comparators (Fig. 3). The output of the comparator has shorter rising and falling time, resulting in a quicker response of the MOS switch and less reverse leakage in the Rectifier1 for analog circuit. An input of the first comparator (Comp1) is one output (V_{ref2}) of the rectifier for digital circuits (Rectifier2) and one input of the RF frontend. An input of the second comparator (Comp2) is the other output (V_{ref1}) of Rectifier2 and the other input of the RF frontend (Fig.3). The source of the comparator is digital source voltage (DVDD).

B. Bio-Sensor Interface

The bio-sensor interface consists of a current splitter, an ADC and a DAQ module. The DAQ consists of a readout circuit to detect weak current signal and a potentiostat.

1) Current splitter. An improved current mirror [8] is designed to obtain sub-pA current. A cascade is introduced to decrease the mismatch of Vds. Simulation under different process corners were conducted and the result presents an error within 2% in all ranges.

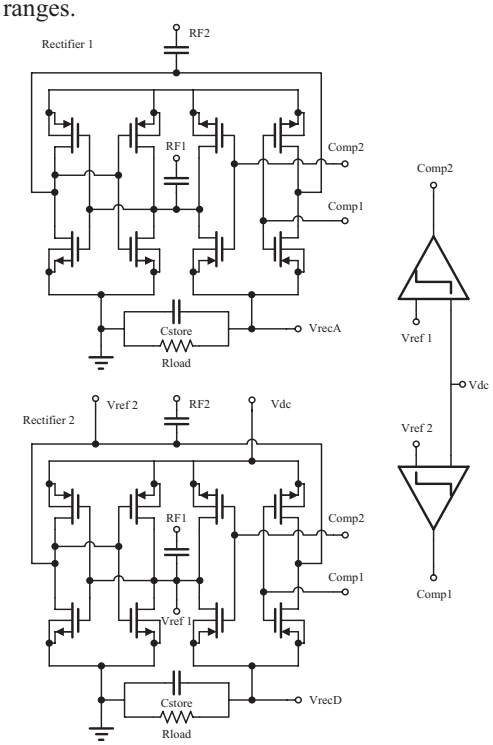

Fig. 3 Schematic of the rectifier

2) ADC. A low power 8-bit SAR ADC structure is designed. The simulation result shows that the ADC has a power consumption of 132.3 nW with a sampling frequency of 10 kHz. The sampling frequency is selected according to the fastest working frequency of the readout circuit in this design. Note that power consumption can be lowered further by organizing different frequencies between integration and S/H in the readout circuit.

3) DAQ. Weak current detection confronts many problems, such as imperfect operation amplifier, leakage current, noises, and so on. In this paper, a readout circuit with CDS is proposed to detect current down to 10 fA. CDS technology is used to reduce the 1/f noise and eliminate the offset of op-amp [9]. Thermal noise is cut by the switch capacitor circuit; the T-Switch is adopted to minimize the leakage current during the "off" state. A detection method of Chronoamperometry will be used to measure the concentration of glucose. The interface circuit works in a discontinuous way to reduce power consumption. An electronic model [10] of the three-electrode-sensor is selected to do the analysis of the loop stability to prevent the possible instability during restart.

a. Current Readout Circuit

The current readout circuit comprises a pre-amp for integration and an S/H circuit, as illustrated in Fig. 4(a). I_{sen} represents the current acquired from the electrochemical sensor. The switches in circuit are controlled by the basic clocks Φ_1, $\overline{\Phi_1}$, Φ_2 and $\overline{\Phi_2}$, shown in Fig. 4(d). The detailed two-phase non-overlapping clocks are designed to lessen the charge injection effect. Under the control of the clocks, the whole circuit works under two main states. In the first state

(Fig. 4(b)), the 1/f noise and offset of the op-amp are sampled by C_s. And in the second state (Fig. 4(c)), the C_s is flipped over and connected to the equivalent voltage of noise and offset. As a result, the noise and the offset are subtracted. Then C_f is charged by the sample current. Assuming the integrating time period is T with a duty cycle of 1 the output of the circuit will be:

$$V_{out} = \frac{I_{sen}}{C_f} * \frac{T}{2} \quad (2)$$

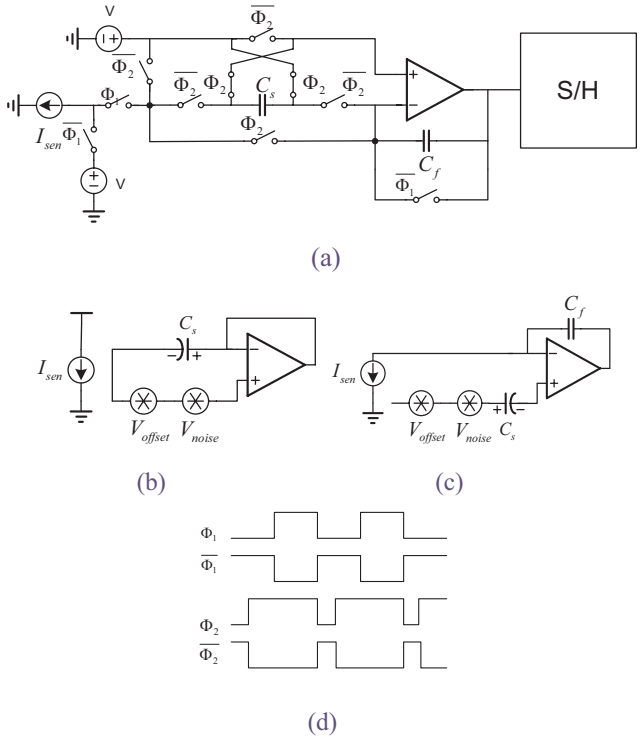

Fig. 4. Schemes of readout circuit: (a) Circuit scheme of the readout circuit (b) State of sampling in CDS (c) State of integration (d) The clocks

Since the value of blood sugar may change significantly, for example, before and after meals. Therefore, the readout circuit has been designed to work in different ranges through the change of working frequency, resulting in four measure ranges, respectively, 10fA-100fA, 100fA-1pA, 1pA-10pA and 10pA-100pA. Different lengths of T are selected to detect different ranges of current. For example, with T=2s, current range of 10f~100f is amplified and transformed to 0.1~1V at the output port correspondingly. A range selection has been designed during detection to ensure the right measurement.

b. T-switch

A T-switch [11] is introduced to cut the leakage currents in MOS switch (Fig. 5). Leakage current of MOS working in weak inversion can be much larger than the detected current 10f during "off" state with a large drain/source voltage. With two additional transistors, N2 and N3, the T-Switch can diminish the drain/source leakage. When it is shut off, meaning the clock Φ is low and clock ~Φ is high. As the MOS N3 works in linear region, node A will be pulled to Voltage V, same as the input port, resulting in little drain/source leakage current. The simulation result shows that the value can be as low as sub-fA.

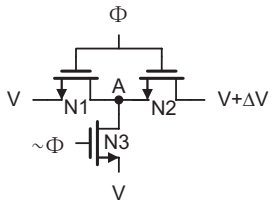

Fig. 5. Scheme of T-Switch

To avoid the possible gate leakage, the thick gate MOS is used. Furthermore, the channel width of the MOS used in T-switch is minimized to cut the reverse PN leakage area in source and drain. The calculation reveals that the reverse diode leakage current of every drain or source diffusion is about 6 aA, which, after a careful evaluation of the circuit in the whole working period, is negligible to detect the current of 10 fA.

Since the implantable chip operates at the temperature between 20℃ and 40℃ and the PSRR of the reference circuits is large enough, P and T could not have an apparent influence. However, the influence of different processes is unavoidable but it can be calibrated by external fuse trimming. Though the voltage error has slight influence on the readout circuit, it may result in considerable impacts on the ADC.

C. Baseband

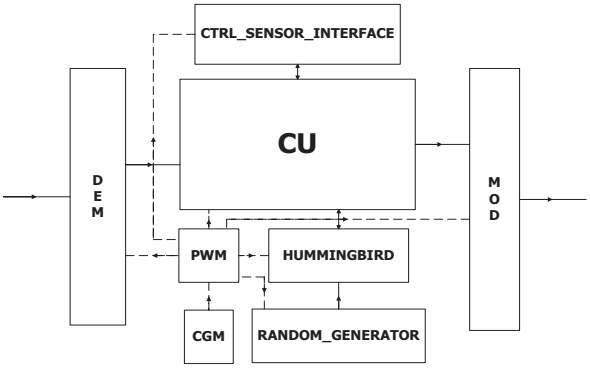

Fig. 6. Diagram of Baseband

The Baseband accomplishes the data processing before and after the transmission between the reader and the sensor tag SoC and provide signals to control the work of the whole chip, including self-calibration during setup and the range selection during detection. The baseband is mainly divided into 6 modules according to their functions (Fig. 6): 1) Clock Generator (CGM), to divide clocks from basic 13.56 MHz; 2) Demodulate Module (DEM), to demodulate data and send SOF, EOF to VCD; 3) Control Unite (CU), to generate control signals for the system, including decoder which decode the command from the reader, FIFO to store the signal from ADC and the data ready to send out, and CRC16 sub module to generate check code and check CRC; 4) Modulate Module (MOD), to send single-carrier modulated data to VCD in fast way; 5) Ctrl_Sensor_Interface Module, to control the DAQ and ADC; 6) Power Management Module (PMW), to realize the management of the power and distribute the clocks of the system.

In order to protect the privacy of the patients, the data stored in baseband is encrypted with the Hummingbird Algorithm [6] before sent to modulator via CU, using a 128-bit key shared by the reader and the sensor tag.

IV. Simulation Results

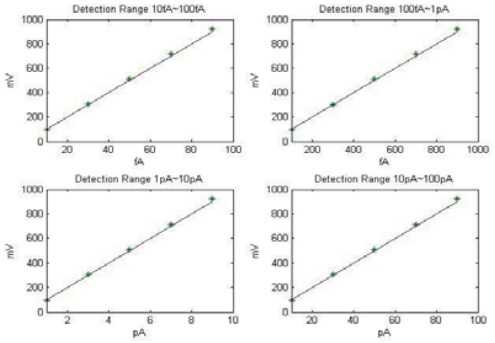

Fig. 7. Simulation results of readout circuit in 4 ranges

The current readout circuit is simulated in different detection ranges (Fig. 7). The lines represent the ideal values and the points represent simulation results. Note that the circuit works well in both linearity and accuracy.

Table I. Properties of each module

	Module	Performance	Power
RF Front-end	Rectifier	Ripple rate<1%; Efficiency>35%; Load capacity=1nF;	N/A
	Bandgap	35ppm/°C	480nW
	LDO	Voltage drop=10mV, PSRR=50dB	10μW
Bio-Sensor Inter-face	Current splitter	2% error in different process corners	556nW
	Readout circuit	Input range 10fA~100pA Output 0.1V~1V;SNR>49dB	13.2 μW
	Potentiostat	PM>70°; Stable within 20ms in transient response	3.6μW
	ADC	8 bit; Sampling rate=10kS/s; FOM=52.93fJ/conv	132nW
Baseband			23μW
Sensor Electrodes		ID=100μm,25μm,10μm; OD=160μm,45μm,25μm	N/A

The performance and the power consumption of every module have been summarized in Table I. The total power consumption after rectifier is 50.968 μW.

The layout of the implantable bio-sensor tag chip has been finished (Fig. 8), with an area of 870 μm × 1,563 μm. To support the research of the sensor, three electrodes with different sizes have been implemented with top metal.

V. Conclutions

A wireless high frequency implantable glucose sensor tag SoC with a novel weak current detection circuit, a crypto engine and on-chip electrodes is proposed in this paper. Simulation results show that the SoC cost less than 100 μW in power consumption and less than 1.2 mm^2 in area and that by using CDS technology and T-Switch the system is able to achieve weak current measurement as low as 10 fA. The chip has been taped out and will be tested soon after we get it back.

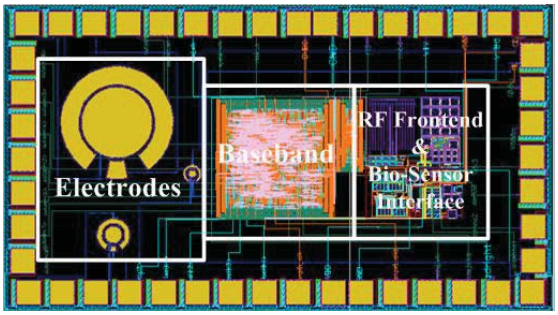

Fig. 8. Layout of the implantable bio-sensor tag chip

References

[1] UK Prospective Diabetes Study (UKPDS) Group,, "Intensive bloodglucose control with sulphonylureas or insulin compared with conventional treatment and risk of complications in patients with type 2 diabetes(UKPDS 33)," The Lancet, vol. 352, no. 9131, pp. 837–853, Sep.1998.

[2] Y. Ohkubo et al., "Intensive insulin therapy prevents the progression of diabetic microvascular complications in Japanese patients with noninsulindependent diabetes mellitus: A randomized prospective six yearstudy," Diabetes Res. Clin. Pract., vol. 28, no.2, pp. 103–117, 1995.

[3] Mohammad Mahdi Ahmadi, Graham A. Jullien, "A wireless-Implantable Microsystem fo Coninuous Glood Glucose Monitoring". IEEE transactions on Biomedical circuits and systems, Vo.3, No. 3, June 2009, pp. 169-180.

[4] Pietro Valdastri, Ekawahyu Susilo, Thilo Forster, Christof Strohhofer, Arianna Menciassi, and Paolo Dario, "Wireless Implantable Electrnoc platform for Chronic Fluorescent-Based Biosensor", IEEE transactions on Biomedical Engineering, Vo.58, No. 6, June 2011, pp. 1846-1854.

[5] ISO/IEC 15693-2 protocol, 2000 (E), www.iso.org.

[6] Meng-Qin Xiao; Xiang Shen; Yu-Qing Yang; Jun-Yu Wang, "Low power implementation of hummingbird cryptographic algorithm for RFID tag". 10th IEEE International Conference on Solid-State and Integrated Circuit Technology (ICSICT), 2010. pp: 581 – 583.

[7] Yue Huang, Andrew J. Mason, "A Redox-Enzyme-Based Electrochemical Biosensor with a CMOS Integrated Bipotentiostat". Biomedical Circuits and Systems Conference, 2009. BioCAS 2009. IEEE,pp29~32

[8] B.L.Barranco and T.S.Gotarredona:" On the Design and Characterization of Femtoampere Current-mode Circuits",Solid-State Circuits, IEEE Journal of , Volume: 38 , Issue: 8, 2003, pp1353~1363

[9] Christian C. Enz, and Gabor C. Temes, "Citcuit Techniques for Reducing the Effects of Op-Amp Imperfections: Autozeroing, Correlated Double Sampling, and Chopper Stabilization", Proceedings of the IEEE, Vol. 84, No. 11, Nov. 1996,pp1584~1641

[10] Bard, Allen J.; Larry R. Faulkner (2000-12-18). Electrochemical Methods: Fundamentals and Applications (2 ed.). Wiley. ISBN 0471043729

[11] Koichi Ishida, Kouichi Kanda, "Managing Subthreshold Leakage in Charge-Based Analog Circuits With Low-Vth Transistors by Analog T-switch and Super Cut-off CMOS", Solid-State Circuits, IEEE Journal of,Volume: 41, Issue: 4, Vol.41 No.4 April 2006, pp859~867.